To appear in ApJ Letters

Diffraction Limited Imaging Spectroscopy of the SgrA* Region using OSIRIS, a new Keck Instrument

A. Krabbe, C. Iserlohe

I. Physikalisches Institut, Universität zu Köln, 50937 Köln, Germany

krabbe@ph1.uni-koeln.de

and

J. E. Larkin, M. Barczys, M. McElwain, J. Weiss, S. A. Wright

Division of Astronomy, University of California, Los Angeles, CA, 90095-1562, USA

and

A. Quirrenbach

Leiden Observatory, P.O. Box 9513, NL-2300 RA Leiden, The Netherlands

ABSTRACT

We present diffraction limited spectroscopic observations of an infrared flare associated with the radio source SgrA*. These are the first results obtained with OSIRIS, the new facility infrared imaging spectrograph for the Keck Observatory operated with the laser guide star adaptive optics system. After subtracting the spectrum of precursor emission at the location of Sgr A*, we find the flare has a spectral index ($F(\nu) \propto \nu^{\alpha}$) of $\alpha = -2.6 \pm 0.9$. If we do not subtract the precursor light, then our spectral index is consistent with earlier observations by Ghez et al. (2005). All observations published so far suggest that the spectral index is a function of the flare's K-band flux.

Subject headings: Spectroscopy: infrared, imaging — Telescopes: Keck — Instruments: OSIRIS — individual(Galactic Center, SgrA*)

1. Introduction

The low luminosity of the Supermassive Black Hole (SBH) in the center of our Galaxy is a standing puzzle and challenges our understanding of the mechanisms of mass accretion as well as the physics close to the event horizon. Infrared variability of SgrA*, first reported by Genzel et al. (2003) and Ghez et al. (2004), has become an important observable. The timescales (few minutes) imply that emission arises from the immediate environment outside of the SBH. Due to the accretion's favorable duty cycle, flares are not only fairly frequent, but they are also readily observable with adaptive optics at 8-10m class telescopes (Clénet et al. 2005; Ghez et al. 2005). The infrared variability is closely linked to the X-ray variability detected a few years earlier (Baganoff et al. 2001; Porquet et al. 2003; Goldwurm et al. 2003). Simultaneous infrared/X-ray observations have demonstrated that the flares are related multiwavelength phenomena (Eckart et al. 2004). The spectral index of the flare and its possible variation from flare to flare and during a single flare are important parameters that will allow us to determine the emission process of the radiation (Yuan et al. 2003, 2004; Liu et al. 2004). We observed SgrA* with OSIRIS, a new Keck facility instrument, during its commissioning time (Larkin et al. 2003; Krabbe et al. 2004; Quirrenbach et al. 2003; Weiss et al. 2002). These data are the first laser guide star (LGS) assisted spectra ever taken of the Galactic Center region.

2. Observations and Data reduction

The OSIRIS (OH Suppressing InfraRed Imaging Spectrograph) instrument is a new facility near infrared (NIR) Z- to K-band imaging spectrograph designed for the Keck Observatory's Adaptive Optics (AO) system. It utilizes an array of micro lenses and a HAWAII-2 detector (2048×2048 pixels) to simultaneously obtain more than 1020 spectra over a rectangular field of view with about 16×64 spatial positions. Each spectrum in this mode covers about 1700 channels at a spectral resolution of R = 3700. OSIRIS achieves high sensitivity with good instrumental throughputs, low backgrounds per AO resolution element and high enough spectral resolution to work between the night sky lines. First light was achieved on February 22, 2005, and commissioning will be completed in 2006. A detailed account of OSIRIS will be given by Larkin et al. (in preparation).

The Galactic Center was observed on April 29, 2005 at Keck II during the first deployment of OSIRIS with the LGS AO system (Wizinowich et al., in prep., van Dam et al., in prep.). Two consecutive K-band frames, each with 300 s integration time were obtained at an airmass of 1.65 with SgrA* in the field of view (FOV). Overhead between the frames was about 37 s. The frames were followed by an empty sky field obtained immediately after the

2^{nd} frame. The angular scale of OSIRIS was set to 20 mas/pixel.

A dedicated OSIRIS data reduction pipeline has been produced, and was used to identically reduce both exposures. After sky subtraction, the individual spectra in each frame were extracted from the raw frame, using a special map of the point spread function of each lenslet at all wavelengths. This allows the removal of crosstalk from adjacent spectra and correct assignment of flux to each field position over the 2-dimensional field. Arc line spectra are used to calibrate the wavelength scale of each field point. Atmospheric differential dispersion effects were also corrected by tracing the peak emission of the stellar continuum through the wavelength slices of the cube. Telluric and instrumental transmission, as well as foreground extinction to the Galactic Center, were corrected in both data cubes by dividing all spectra by the average spectrum of star S2. All spectra were finally multiplied by a black-body curve of T = 30000 K, representing the approximate flux density of S2 which is assumed to be between spectral classes O8V and B0V based on spectra from Ghez et al. (2003). Since we didn't attempt to model the stellar absorption lines, e.g., Brγ at 2.166 μm, the final spectra do not contain valid information about emission or absorption lines at those spectral positions and were ignored in our analysis.

3. Results

Figure 1 has two panels, hereafter referred to as frame 1 and frame 2, that display the image produced by collapsing all of the wavelength channels from 2.02 μm through 2.38 μm for each of the two frames. Some of the stars are labeled according to Eisenhauer et al. (2005). Frame 2 was observed 0.3″ south with respect to Frame 1. The angular resolution on the sky is 60 mas at a pixel scale of 20 mas. The angular resolution achieved is worse than the diffraction limit of 46 mas at 2.18 μm, probably due to the low telescope elevation.

The staggered edge along the sides of each data cube is standard for OSIRIS and is due to the complex mapping of lenslets onto the detector. Due to constraints in the commissioning schedule, a global flat was not available for these observations. This means that individual spatial locations have a well calibrated spectrum, but based on comparisons of known stellar fluxes in the field, the relative intensity of one spectrum to another is uncertain at the 20% level (reflected in the flux errors in Table 1). Star S2 has a well determined flux and was used to flux calibrate both frames individually.

The flare at the position of SgrA* is apparent in frame 2. It is located 145±5 mas south and 22±5 mas west of S2 at the epoch of the observations: MJD53489.624680. Inspecting the identical position in frame 1 reveals a weaker but still notable emission at the location

of Sgr A*, which we will term the precursor. In both frames, the emission is close to other stars making a proper background subtraction important and slightly difficult. The levels and spectra of the backgrounds at SgrA* and S2 are certainly not identical and had to be treated individually. In the end the spectrum of SgrA* was determined from frame 2 using a 5 pixel × 4 pixel box centered on the position of the flare. The general background was determined by measuring the average pixel value in the 22 pixels that form a circumference around the 5×4 aperture. The spectrum of S2 was determined in an identical fashion from the same frame, in order to reduce systematic errors that could result from using different fractions of the point spread function or by measuring the background in a different manner. An identical procedure was applied to frame 1 to extract the precursor spectrum, except a 5×5 pixel aperture was used due to a fractional shift of the lenslet grid on the sky between frames 2 and 1. Again, the size and geometry of the box was identical to that used for the extraction of the S2 spectrum discussed earlier. Assuming that the flare is unresolved in our data, the extraction regions for SgrA* and star S2 then cover the same fraction of the PSF for each source.

The resulting spectra are shown in Figure 2. The lowest spectrum represents the precursor emission in frame 1. The middle spectrum is the extracted spectrum of the flare from frame 2, and has has been shifted vertically by one unit for clarity. The upper spectrum is the difference between the spectrum in frame 2 and the spectrum in frame 1, and we will refer to this as the flare spectrum. Again for clarity, it has been shifted vertically by 4 units. All three of the spectra have been smoothed by a 30 pixel wide boxcar filter. The sky frame was obtained after both frames 1 and 2 and was a poorer match for frame 1. This was particularly important in the spectral range between 2.04 μm and 2.06 μm and this region was masked out in frame 1. Atmospheric OH lines, however, subtracted out well. All three of the spectra were fit with a power law ($F(\lambda) \propto \lambda^m$) and the resulting fits and slopes (m) are given on Figure 2 along with 1σ errors. These slopes were converted into a frequency power law index α ($F_\nu \propto \nu^\alpha$). Table 1 shows all of the derived quantities including the slope and spectral index. We note here that the spectral index of the flare is quite red ($\alpha = -2.6 \pm 0.9$).

From the spectral fits, the K-band flux of the flare and the precursor were determined relative to S2 by extrapolating the power law fit from (2.02 μm, 2.38 μm) to the full K-band. We assumed that S2 has a magnitude of $m_K = 13.9$ mag (24 mJy) based on photometry from Ghez et al. (2003). The K-band flux of the precursor emission at the location of SgrA* in frame 1 then becomes 3.5 mJy, or 6.9 times fainter than S2. The corresponding flux at the location of Sgr A* in frame 2 is 9.6 mJy, or 2.5 times fainter than S2. This is an increase in the K-band flux of SgrA* by a factor of 2.8 within 5.6 minutes (exposure time plus overhead between frames).

4. Discussion and Summary

While frame 2 (Fig. 1b) obviously shows a flare at the position of SgrA*, it is less clear what is at the same location in frame 1 (Fig 1a). Is it a true quiet state or a mild flare precursor? A faint source at the location of SgrA* has been found by other observers, including in high resolution H-band images by Eisenhauer et al. (2005) with the NACO instrument. Photometric K-band data by Genzel et al (2003) indicate that SgrA* can be more than 6 times fainter than S2. Eckart et al. (2004) report the lowest activity level 12 times fainter than S2 corresponding to a K-band flux density of 2 mJy. Comparing this factor with Table 1 suggests that the K-band emission in frame 1 is less than a factor of 2 brighter than the lowest activity level measured and may indeed be dominated by an underlying constant source. The spectral index of the source in frame 1 (α=2.7 $\pm$ 1.3) is also consistent with a blackbody at a temperature around 3000 K. This suggests the possibility that the emission at the location of SgrA* during low activity may be dominated by a different mechanism than the flare itself. One option is a stellar component either in the background or at the very cusp of the stellar cluster within less than a light day of SgrA*. If this is the case, then these faint stars are also orbiting in the immediate vicinity of SgrA*.

The temporal separation between the two frames is 337 seconds (exposure times of 300 sec with a gap of 37 seconds). Within this time or shorter, the K-band flux increased by more than a magnitude to 9.6 mJy. This peak flux compares very well with Eckart et al. (2004) and also with Ghez et al. (2005) for the maximum observed activity. Our observations thus very likely record the beginning of a flare with a typical level of activity. We also conclude that the intrinsic K-band flux of the flare is probably best represented by the difference between the peak value of 9.6 mJy and the lowest background of 2 mJy, yielding (7.6 $\pm$ 34%) mJy. This value has been used in Figure 3.

Eisenhauer et al. (2005) were first to report measurements of the spectral index of the emission of SgrA* in the NIR. Their spectral indices α for the flux density F_ν lie in the range between -3.3 and -4.8, with an averaged index of $\alpha_E = -4 \pm 1$ for fluxes < 2 mJy. Their value has been obtained in a similar fashion to ours, in that two spectra of different activity levels were subtracted from each other. However, their result is different from our value of $\alpha_K = -2.6 \pm 0.9$ (see Table 1 and Figure 3).

Figure 3 summarizes all published spectral indices for SgrA*'s K-band flares as a function of their 2 μm flux density. In a recent paper, Ghez et al. (2005) report spectral indices based on K$'$ and L$'$ imaging. Their method of determining α is directly based on K$'$-L$'$ PSF fitting photometry. However, different from our result and from Eisenhauer et al. (2005), their result does not account for flux from the precursor source. Thus their value of α = -0.5 has a different meaning than our flare index. It is more correctly compared to the slope of the

spectrum in frame 2 which includes the local background and has an index of $\alpha = -0.6 \pm 0.4$, consistent with the Ghez measurement. In addition, their K-band flux densities are close to our results, especially if we correct for the difference between K′ and K bands. Using their spectral index value of α = -0.5 and K′ flux density of 7.2 mJy, we calculate a K-band flux density of 9.2 mJy, again very comparable to our measurement of 9.6 mJy for frame 2.

We thus confirm the findings of Ghez et al. (2005) for the slope of the flare plus local background within the 1 σ errors. It is interesting to note that both spectral indices were obtained by very different techniques and using different wavebands: K′ and L′ versus K band only. The spectral indices reported by Eisenhauer et al. (2005) are clearly different but were also taken at a significantly lower level of activity. A possible interpretation of the difference in spectral index as a spectral break between 2.4 and 3.8 μmwas first suggested by Ghez et al. (2005). Our new data show that the K-band spectrum has a smooth constant spectral slope. The spectral slope of our data is close to the Ghez et al. value, leaving little room for a spectral break between 2.4 and 3.8 μm. Instead, taken at face value, our data imply a dependency of the spectral index on the flare intensity, another suggestion first made by Ghez et al. (2005). This same conclusion has also been reached by Gillessen et al. (2006) based on near infrared spectra taken with the SINFONI instrument at the VLT.

Theoretical models by Yuan et al. (2004) and Liu et al. (2004) indicate that both the infrared and the X-ray variability is probably due to hot or relativistic gas accelerated at $\sim$ 10 times the Schwarzschild radius, R_S. The synchrotron emission from the high-energy electrons within this gas accounts for the observed X-ray flares. The models can also be tuned to explain the infrared flux and its variability. The models are flexible enough to produce spectral indices between -2.0 and -3.0, consistent with measurements from this paper (see Figure 4 of Yuan et al. (2003)). We note that both Yuan et al. (2004) and Liu et al. (2004) explicitly mention that varying spectral indices may be a feature of such flares. More spectroscopic data at different flare intensity levels are needed to confirm such a trend. If the flare spectral index is a function of the flare activity level, it favors a model in which stronger flares involve more energetic electrons, making the infrared spectrum bluer. Such a finding would considerably narrow the range of process parameters describing the origin of the flare.

The authors would like to sincerely thank the dedicated members of the OSIRIS engineering team: Ted Aliado, George Brims, John Canfield, Thomas Gasaway, Chris Johnson, Evan Kress, David LaFreniere, Ken Magnone, Nick Magnone, Juleen Moon, Gunnar Skulason, and Michael Spencer. We would also like to thank the Keck Observatory Staff (CARA) who were part of the OSIRIS team and helped with commissioning. Special thanks goes to Cara staff members Sean Adkins, Paola Amico, Randy Campbell, Al Conrad, Allan Honey,

David Le Mignant, Marcos Van Dam, and Peter Wizinowich.

The authors would like to acknowledge the support of the Keck Observatory and the Keck Science Steering Committee. The design and construction of OSIRIS were supported by a grant from the California Association for Research in Astronomy, which owns and operates the Keck Observatory. A major portion of the CARA funds were provided by the TSIP program from the National Science Foundation. This work also received early support from the National Science Foundation Science and Technology Center for Adaptive Optics (CfAO), managed by the University of California at Santa Cruz under cooperative agreement No. AST-98-76783.

Facilities: Keck (OSIRIS)

REFERENCES

Baganoff, F.K., et al. 2001, Nature, 413, 45

Clénet Y., Rouan D., Gratadour, D., Marco, O., Léna, P., Ageorges N., & Gendron, E. 2005, A&A, 439, L9

Eisenhauer, F., Genzel, R., Alexander, T., Abuter, R., Paumard, T., et al. 2005, ApJ, 628, 246

Eckart, A., Baganoff, F.K., Morris, M., Bautz, M.W., Brandt, W.N., et al. 2004, A&A, 427, 1

Genzel R., Schödel, R., Ott T., Eckart, A., Alexander, T., et al. 2003, Nature, 425, 934

Ghez, A.M., Duchêne, G., Matthews, K., Hornstein, S.D., Tanner A., et al. 2003, ApJ, 586, L127

Ghez, A.M., Wright, S.A., Matthews, K., Thompson, D., Le Mignant, D., et al. 2004, ApJ, 601, L159

Ghez, A.M., Hornstein, S.D., Lu, J., Bouchez, A., Le Mignant, et al. 2005, ApJ, 635, in print

Gillesen, S., Eisenhauer, F., Quataert, E., Genzel, R., Paumard, T., Trippe, S., Ott, T., Abuter, R., Eckart, A., Lagage, P.O., Lehnert, M.D., Tacconi, L.J., Martins, F. 2006, ApJ, accepted

Goldwurm, A., Brion, E., Goldoni, P., Ferrando, P., Daigne, F., Decourchelle, A., Warwick, R.S., & Predehl, P. 2003, ApJ, 584, 751

Krabbe, A., Gasaway, T., Song, I., Iserlohe, C., Weiss, J., et al. 2004, SPIE, 5492, 1403

Larkin, J.E., Quirrenbach, A., Krabbe, A., Aliado, T., Barczys, M., et al. 2003, SPIE, 4841, 1600

Liu, S., Petrosian, V., & Melia F. 2004, ApJ, 611, L101

Porquet, D., Predehl, P., Aschenbach, B., Grosso, N., Goldwurm, A., Goldoni, P., Warwick, R.S., & Decourchelle, A. 2003, A&A, 407, L17

Quirrenbach, A., Larkin, J.E., Krabbe, A., Barczys, M., & LaFreniere, D. 2003, SPIE, 4841, 1493

Yuan, F., Quataert, E., & Narayan R. 2003, ApJ, 598,301

Yuan, F., Quataert, E., & Narayan R. 2004, ApJ, 606, 894

Weiss, J., Barczys, M., Larkin, J.E., LaFreniere, D., Quirrenbach, A., et al. 2002, SPIE, 4848, 519

Table 1: Derived Quantities

Target	K [mag]	Spectral slope m ($F(\lambda) \propto \lambda^m$)	F_ν [mJy] [c]	Spectral Index α ($F_\nu \propto \nu^\alpha$)
Star S2 (both frames)	13.9[a]		24	
SgrA* (frame 1)	16.0 ± 0.2[b]	-4.7 ± 1.3	$3.5 \pm 20\%$	2.7 ± 1.3
SgrA* (frame 2)	14.9 ± 0.2[b]	-1.4 ± 0.4	$9.6 \pm 20\%$	-0.6 ± 0.4
SgrA* flare	15.4 ± 0.3[b]	0.6 ± 0.9	$6.1 \pm 34\%$	-2.6 ± 0.9

[a] Ghez et al. (2003). No errors were provided.

[b] Fit extrapolated from (2.02μm – 2.38μm) to full K-band (1.95 μm - 2.40 μm)

[c] $A_K = 2.8 mag$ extinction corrected, Genzel et al. (2003)

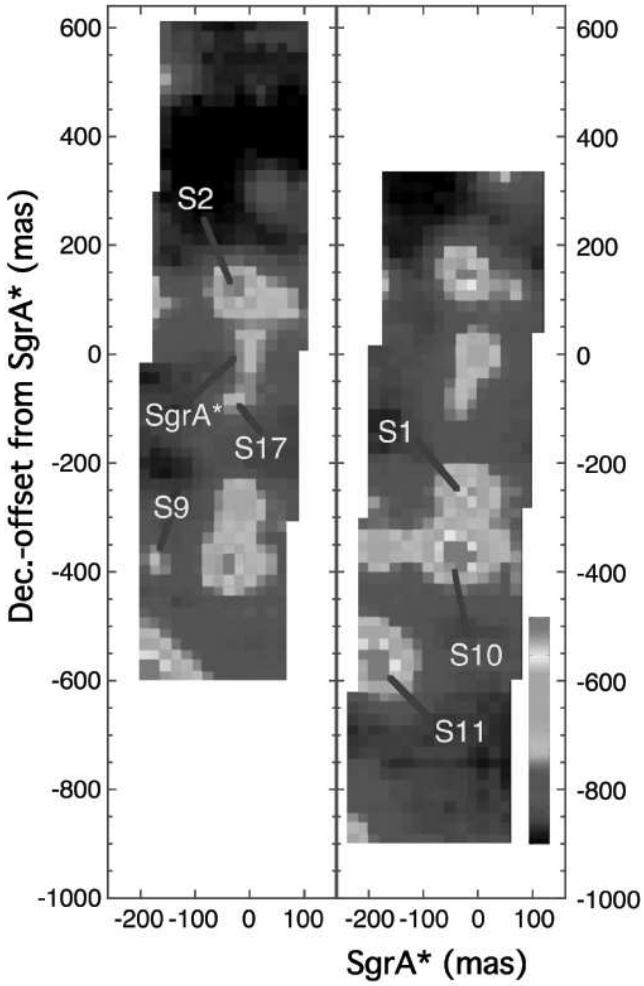

Fig. 1.— K-band images of the immediate vicinity of SgrA*, produced by collapsing the spectral cubes between wavelengths of 2.02 μm and 2.38 μm . Each frame is five minutes long and was obtained sequentially with the Keck II LGS AO system. The data in the right panel are shifted 0.3″ south of those in the left panel. The image scale is 20 mas/pixel and the stellar images have a FWHM of approximately 60 mas, close to the diffraction limit of the Keck II telescope. Some of the stars have been labeled according to Eisenhauer et al. (2005). The position of SgrA* is indicated at (0,0) in both panels. Both frames are not calibrated with respect to each other. However, the flare at the location of SgrA* is clearly significantly brighter in the right panel.

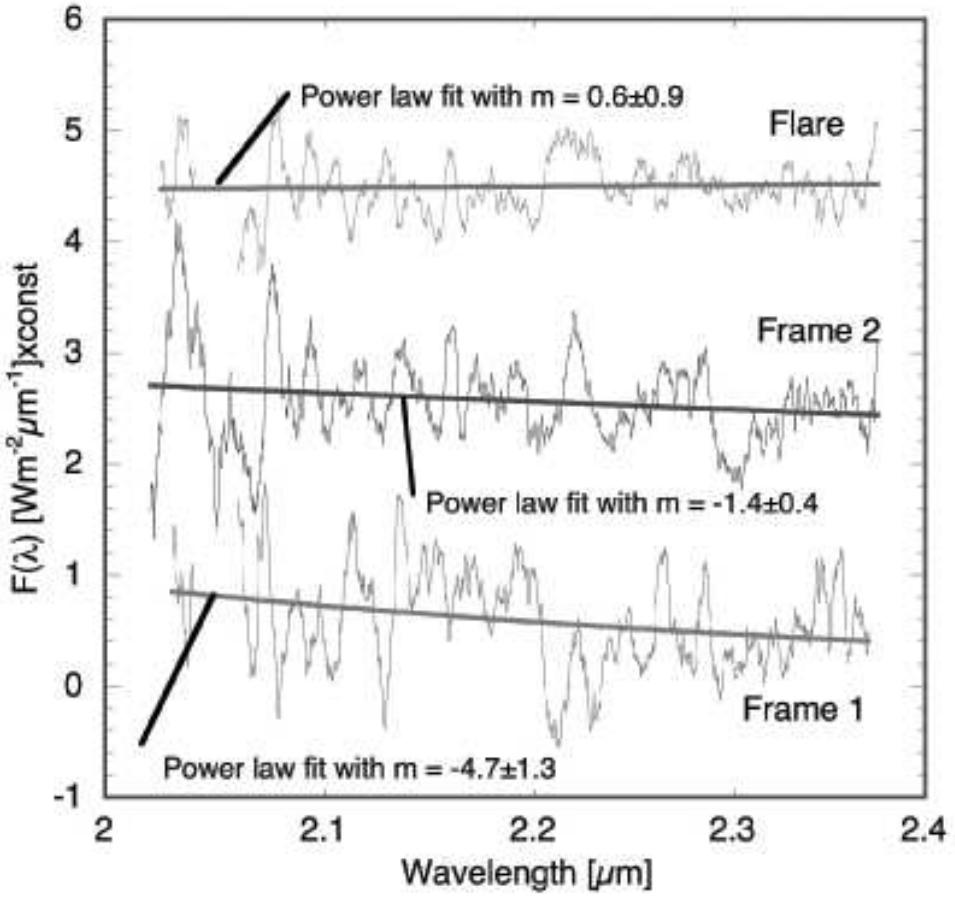

Fig. 2.— Spectra at the location of SgrA* obtained from frame 1 (bottom) and frame 2 (middle) tied to the left axis. The middle spectrum has been shifted up one unit for clarity. The upper spectrum is the difference of the lower two spectra and is referred to as the flare in the text. It has been shifted up by four units. The spectra have been smoothed with a 30 pixel wide boxcar filter for display. The lines represent power law fits to the unsmoothed continua of the spectra. The derived values for the slopes($F(\lambda) \propto \lambda^m$) are indicated.

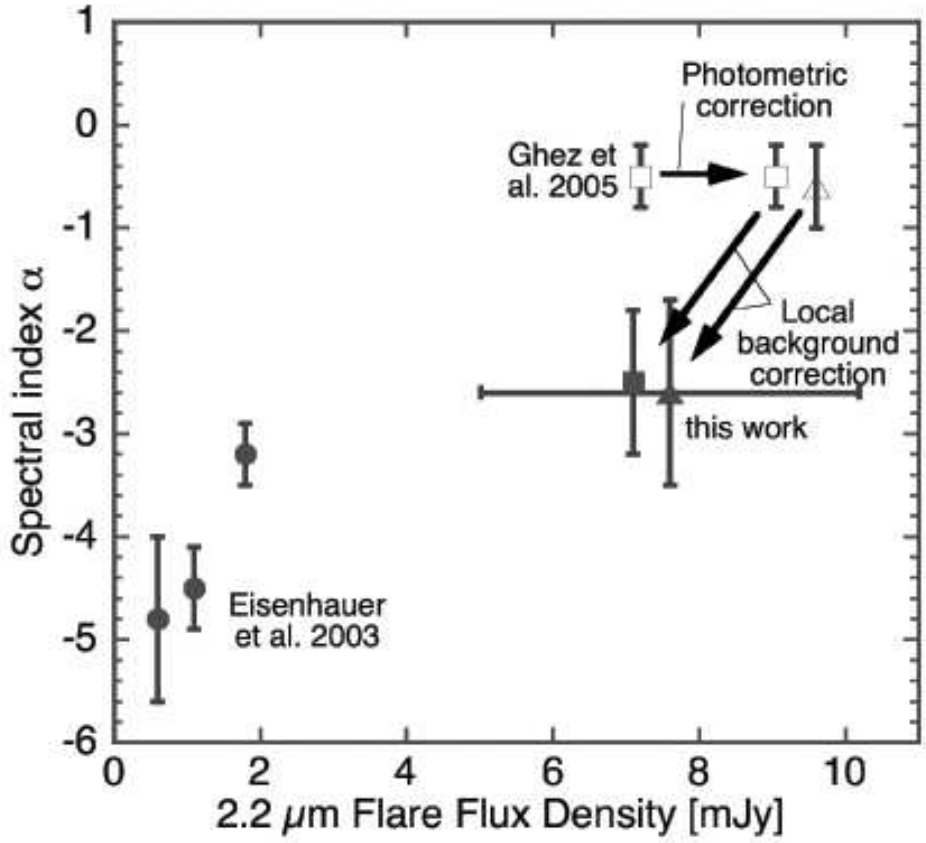

Fig. 3.— SgrA*'s K-band spectral index (α, where $F(\nu) \sim \nu^{\alpha}$) as a function of its 2 μm flux density. The results of Eisenhauer et al. (2005) and Ghez et al. (2005) are indicated. The result of this work are denoted by the triangles. The open triangle marks the spectral index and flux density derived from the spectrum of frame 2 (Fig. 2 middle), the filled triangle represents the flare spectrum (Fig. 2 top) after subtracting the local background (precursor) flux. The top arrow denotes the horizontal shift of the Ghez et al. (2005) data if we use their spectral index measurement to adjust between their observed K$'$ band to our K band (see text) flux. Since the Ghez et al. (2005) data point does not subtract a possible precursor component, and because we do not know the L$'$ band brightness of the precursor, we instead use our measured spectral shape in frame 1 in order to make a plausible estimate of their spectral index without precursor. The shift is indicated by the parallel arrows.